Characterization of the Dizocilpine Binding Site on the Nicotinic Acetylcholine Receptor

HUGO R. ARIAS, ELIZABETH A. MCCARDY, and MICHAEL P. BLANTON

Departments of Pharmacology and Anesthesiology, School of Medicine, Texas Tech University Health Sciences Center, Lubbock, Texas

ABSTRACT

Although the dissociative anesthetic dizocilpine [(+)-MK-801] inhibits nicotinic acetylcholine receptor (AChR) function in a noncompetitive manner, the location of the dizocilpine binding site(s) has yet to be clearly established. Thus, to characterize the binding site for dizocilpine on the AChR we examined 1) the dissociation constant (K_d) and stoichiometry of [^{3}H]dizocilpine binding; 2) the displacement of dizocilpine radioligand binding by noncompetitive inhibitors (NCIs) and conversely dizocilpine displacement of fluorescent and radiolabeled NCIs from their respective high-affinity binding sites on the AChR; and 3) photoaffinity labeling of the AChR using ^{125}I-dizocilpine. The results establish that one high-affinity ($K_d = 4.8 \mu$M) and several (3–6) low-affinity ($K_d = \sim 140 \mu$M) binding sites exist for dizocilpine on the desensitized and resting AChR, respectively. The bind-
ing of the fluorescent NCIs ethidium, quinacrine, and crystal violet as well as [^{3}H]thienylcyclohexylpiperidine was inhibited by dizocilpine on desensitized AChRs. However, Schild-type analyses indicate that only the inhibition of quinacrine in the desensitized state seems to be mediated by a mutually exclusive action. Photoaffinity labeling of the AChR by ^{125}I-dizocilpine was primarily restricted to the $\alpha1$ subunit and subsequent mapping revealed that the principal sites of labeling are localized to the M4 ($\sim$70%) and M1 (30%) transmembrane domains. Collectively, the data indicate that the high-affinity dizocilpine binding site is not located in the lumen of the ion channel but probably near the quinacrine binding locus at a nonluminal domain in the AChR desensitized state.

The muscle-type nicotinic acetylcholine receptor (AChR) is the archetype of the ligand-gated ion channel receptor superfamily. This receptor superfamily includes the neuronal-type AChRs as well as types A and C γ-aminobutyric acid, 5-hydroxytryptamine type 3, and glycine receptors (for reviews, see Changeux and Edelstein, 1998; Arias, 2000). This superfamily is important in mediating synaptic transmission in the nervous system and contributes to higher order brain mechanisms such as memory, learning, perception, cognition, and emotion. The malfunctioning of these receptors has been considered as the origin of several neuropsychiatric disorders.

One of the reasons by which these receptors are considered a superfamily is the existence of high homology between the amino acid sequences of each receptor subunit (Ortells and Lunt, 1995). A second characteristic is that each receptor is formed by five subunits arranged pseudosymetrically around an axis that passes through an ion pore, perpendicular to the plane of the membrane [reviewed in Changeux and Edelstein (1998) and Arias (2000)]. A third feature, shared by all members, is that each subunit can be divided in three structurally different but functionally interrelated portions: 1) the extracellular portion, where two binding sites for the respective neurotransmitter are located at the interfaces of two subunits; 2) the transmembrane portion, comprising the M1–M4 domains, where M2 from each subunit forms the ion channel wall; and 3) the cytoplasmic portion, where several phosphorylation sites exist.

In addition to this receptor superfamily, other neurotransmitter-gated ion channels such as the receptors for glutamate (GluR) and for ATP have been found (for reviews, see Changeux and Edelstein, 1998; Arias, 2000). Nevertheless, both receptor families present several structural characteristics that make them distinct from that comprising the AChR and their cousins. For example, the GluR is formed by four subunits, each one containing an agonist binding site located at the interface of two extracellular lobes as well as

ABBREVIATIONS: AChR, nicotinic acetylcholine receptor; GluR, glutamate receptor; NMDA, *N*-methyl-D-aspartate; PCP, phencyclidine; TCP, thienylcyclohexylpiperidine; (+)-MK-801, dizocilpine maleate [(5*R*,10*S*)-(+)-5-methyl-10,11-dihydro-5*H*-dibenzo[*a,d*]cyclo-hepten-5,10-imine hydrogen maleate]; CCh, carbamylcholine; TMB-8, 3,4,5-trimethoxybenzoic acid 8-(diethylamino)octyl ester hydrochloride; α-BTx, α-bungarotoxin; Tricine, *N*-[2-hydroxy-1,1-bis(hydroxy, ethyl)ethyl]glycine; CrV, crystal violet; VDB, vesicle dialysis buffer; MOPS, 4-morpholinepropanesulfonic acid; RT, room temperature; NCI, noncompetitive inhibitor; PAGE, polyacrylamide gel electrophoresis; HPLC, high-performance liquid chromatography; HTX, histrionicotoxin; [^{125}I]TID, 3-fluoromethyl-3-(*m*-[^{125}I]iodophenyl)diazirine.

three transmembrane domains (M1, M3, and M4) and a reentrant membrane loop. The GluR family, which mediates fast excitatory transmission in the central nervous system, can be classified according to their selective agonists: the *N*-methyl-D-aspartate (NMDA), the kainate, and the α-amino-3-hydroxy-5-methyl-4-isoxazole propionate receptor types. Although the NMDA receptor and the AChRs are not structurally related, they share certain pharmacological properties such as the noncompetitive inhibition elicited by a number of different dissociative anesthetics, including phencyclidine (PCP) and its structural analog thienylcyclohexylpiperidine (TCP), ketamine, and dizocilpine (for review, see Arias, 1998; Krasowski and Harrison, 1999). In this regard, dizocilpine inhibits both receptor classes by binding to sites located in a domain different from that for each specific neurotransmitter (Ramoa et al., 1990; Amador and Dani, 1991). Although dizocilipine is reported to be an open-channel blocker of α4β2 neuronal nicotinic AChRs (Buisson and Bertrand, 1998), studies examining the mechanism of receptor inhibition (Grewer and Hess, 1999) as well as the lack of stereoselectivity for the inhibition of α7 AChRs (Briggs and McKenna, 1996) suggest that dizocilpine inhibition may not simply result from steric blockade of open-channel AChRs.

This work is an attempt to characterize the binding site of the dissociative anesthetic and anticonvulsant dizocilpine [(+)-MK-801] on the *Torpedo californica* AChR. For this purpose, we will use fluorescence spectroscopy, photoaffinity labeling, and radiochemical techniques as well as Schild-type analyses. AChR native membranes from *T. californica* electric organ can be obtained at high specific activity (1–2 nmol/mg protein); thus, this preparation will permit the examination of anesthetic binding sites not detectable in the central nervous system where the specific activity for neuronal AChRs is more than 10,000 lower.

Experimental Procedures

Materials. Piperidyl-[3,4-³H(N)](*N*-(1-(2 thienyl)cyclohexyl)-3,4-piperidine) ([³H]TCP; 57.6 Ci/mmol), (+)-[3-³H]dizocilpine (21.7 Ci/mmol), and (+)-3-¹²⁵I-dizocilpine (2200 Ci/mmol) were purchased from PerkinElmer Life Sciences Products, Inc. (Boston, MA) and stored at −20°C. Quinacrine dihydrochloride, suberyldicholine dichloride, carbamylcholine chloride (CCh), dizocilpine maleate [(+)-MK-801], proadifen, 3,4,5-trimethoxybenzoic acid 8-(diethylamino)octyl ester hydrochloride (TMB-8), TCP, PCP, α-bungarotoxin (α-BTx), and Tricine were purchased from Sigma Chemical Co. (St. Louis, MO). Ethidium bromide and Genapol C-100 were purchased from Calbiochem (La Jolla, CA). Crystal violet hydrochloride (CrV) was obtained from Aldrich Chemical Company, Inc. (Milwaukee, WI). [1-(Dimethylamino) naphtalene-5-sulfonamido]ethyltrimethylammonium perchlorate (dansyltrimethylamine) was obtained from Pierce Chemical Co. (Rockford, IL). *Staphylococcus aureus* V8 protease was obtained from ICN Biochemicals (Costa Mesa, CA). L-1-Tosylamido-2-phenylethylchloromethyl ketone-treated trypsin came from Worthington (Lakewood, NJ). Other organic chemicals were of the highest purity available.

Preparation of Membranes. AChR-rich membranes were prepared from frozen *T. californica* electric organs obtained from Aquatic Research Consultants (San Pedro, CA) by differential and sucrose density gradient centrifugation, as described previously (Pedersen et al., 1986). The specific activities of these membrane preparations were determined by the decrease in dansyltrimethylamine (6.6 μM) fluorescence produced by the titration of suberyldicholine into receptor suspensions (0.3 mg/ml) in the presence of 200

μM proadifen and ranged between 1.1 and 1.6 nmol of suberyldicholine binding sites/mg total protein. Considering that the AChR bears two suberyldicholine binding sites, the actual specific activity would be 0.55 to 0.80 nmol of AChR/mg of protein. The AChR membrane preparations (in 36% sucrose, 0.02% NaN₃) were stored at −80°C.

Fluorescence Measurements. All fluorescence titrations were carried out with 0.5 × 0.5-cm quartz cuvettes in a SLM-Aminco-Bowman Series 2 luminescence spectrometer. Quinacrine excitation and emission wavelengths were 450 and 502 nm, respectively. To reduce stray-light effects a 450-nm narrow band and a 495-nm cutoff filter was placed in the path of excitation and emission beams, respectively. Ethidium excitation and emission wavelengths were 520 and 595 nm, respectively. To reduce stray-light effects a 520-nm narrow band and a 550-nm cutoff filter was placed in the path of excitation and emission beams, respectively. Crystal violet excitation and emission wavelengths were 600 and 645 nm, respectively. To reduce stray-light effects a 600-nm narrow band and a 630-nm cutoff filter was placed in the path of excitation and emission beams, respectively. Dansyltrimethylamine excitation and emission wavelengths were 280 and 546 nm, respectively. To reduce stray-light effects a 530-nm cutoff filter was placed in the path of its emission beam.

Effect of Dizocilpine on Quinacrine, Ethidium, and Crystal Violet Binding. To determine the effect of dizocilpine on quinacrine, ethidium, and CrV association properties, the effect of dizocilpine on the apparent dissociation constant (K_d) of quinacrine, ethidium, or CrV binding was measured as described previously (Valenzuela et al., 1992; Arias et al., 1993a,b; Arias, 1997, 1999a). Additionally, direct titrations of CrV into AChR suspensions (0.3 μM) in vesicle dialysis buffer (VDB; 10 mM MOPS, 100 mM NaCl, 0.1 mM EDTA, and 0.02% NaN₃, pH 7.5), without CCh, in the absence or in the presence of PCP (100 μM), and different concentrations of dizocilpine to determine the apparent K_d values in the resting state were assessed. In this case, PCP was added for the same reason as proadifen was used in the AChR desensitized state experiments, to define the specific or PCP-sensitive fluorescence associated with the binding of CrV to its high-affinity site. The AChR native membrane suspension containing dizocilpine was incubated for at least 2 h (up to 4 h) at room temperature (RT) before the beginning of the titration. Stock solutions of dizocilpine were prepared in VDB at 0.3 mM or in ethanol at 20 mM final concentration.

Estimates of the apparent K_d values of the NCIs were made by fitting the plots of the specific (proadifen- or PCP-sensitive) changes in NCI fluorescence versus added ligand concentration to a four-parameter logistic equation (sigmoid) by means of the Prism program (GraphPAD Software, San Diego, CA).

To determine the inhibition constant (K_i) of dizocilpine from the fluorescent NCI displacement experiments, a Schild-type plot was used according to the equation (Schild, 1949):

$$\log[(K_d^{\text{dizocilpine}}/K_d) - 1] = \log(\text{pA}_2) - \log K_i \qquad (1)$$

where K_d and $K_d^{\text{dizocilpine}}$ are the apparent dissociation constants of the fluorescent NCI in the absence or in the presence of a certain concentration of dizocilpine, respectively, and pA₂ is the negative logarithm of the concentration of dizocilpine that reduces the apparent affinity of either fluorescent NCI by a factor of 2. In other words, when $K_d^{\text{dizocilpine}} = 2K_d$ then, $\log[(K_d^{\text{dizocilpine}}/K_d) - 1] = 0$, and $\log(\text{pA}_2) = -\log K_i$. In this regard, the K_i value can be graphically calculated as the antilog of the *x*-intercept (when y = 0) from the $\log[(K_d^{\text{dizocilpine}}/K_d) - 1]$ versus log[dizocilpine] plot. To determine whether a steric or an allosteric mechanism elicits the observed displacement, the slope of the Schild plot was also considered. A slope of 1 or near unity is indicative of a steric mechanism, whereas a slope value far from unity suggests an allosteric-type of inhibition.

Comparison between Dizocilpine, Quinacrine, and TMB-8 on the Displacement of [³H]TCP or ¹²⁵I-Dizocilpine from Its Binding Site on the AChR. To compare the effects of dizocilpine,

quinacrine, or TMB-8 on the maximum binding of [³H]TCP, ¹²⁵I-, or ³H-labeled dizocilpine to desensitized AChRs, 0.2 μM AChR native membranes were suspended in 8 ml of VDB with either ~6 nM [³H]TCP, ~0.7 nM ¹²⁵I-dizocilpine, or 15 to 36 nM [³H]dizocilpine in the presence of 0.4 mM CCh. Then, the total volume was divided into 16 aliquots, and increasing concentrations of dizocilpine, quinacrine, or TMB-8 were added to each tube and incubated for 2.5 h at RT. After centrifugation (18,000 rpm for 1 h in a JA-20 rotor) of the samples in a Beckman J2-HS centrifuge, the ³H-containing pellets were resuspended in 100 μl of 10% SDS and transferred to a scintillation vial with 5 ml of Bio-Safe II (Research Products International Corp., Mount Prospect, IL). The bound fraction was determined by scintillation counting in a Packard 1900 TR. For ¹²⁵I-dizocilpine binding experiments, the radioactivity in the pellets was directly measured using a Packard Cobra II gamma counter. The nonspecific binding was determined in the presence of 200 μM proadifen. The concentration-response data were curve-fitted by nonlinear least-squares analysis (one-site competition) using the graphical program Prism (GraphPAD). Because the plot for the [³H] and ¹²⁵I-dizocilpine competition experiments does not fit well when Hill coefficients (n_H) near 1 are used, a value that gave the best fit was used instead (Table 2). The 50% drug-induced inhibition of maximal binding of radiolabeled NCIs defines the IC_{50} value for either dizocilpine, quinacrine, or TMB-8. Taking into account that the AChR presents a single high-affinity binding site either for TCP (Katz et al., 1997, and references therein), for quinacrine (Arias et al., 1993a), or for dizocilpine (this article), the observed IC_{50} values were transformed in K_i values using the Cheng-Prusoff relationship (Cheng and Prusoff, 1973):

$$K_i = IC_{50}/\{1 + ([NCI]/K_d^{NCI})\} \tag{2}$$

where [NCI] is the initial concentration of the labeled NCI ([³H]TCP, [³H] or ¹²⁵I-dizocilpine) and K_d^{NCI} is the dissociation constant for TCP (~0.2 μM; Katz et al., 1997) or dizocilpine (4.8 μM; Table 1), respectively. Because the initial concentration of the labeled NCI is in the nanomolar range and their K_d values are in the micromolar concentration range, the calculated K_i values, summarized in Table 2, were practically the same as the initial IC_{50} values.

Equilibrium Binding of [³H]Dizocilpine. The binding [³H]dizocilpine to AChR native membranes was determined by a centrifugation assay similar to that described for [³H]PCP binding (Arias, 1999a). The [³H]dizocilpine/dizocilpine concentration ratio was less than 0.0002; thus, the actual dizocilpine concentration ([³H]dizocilpine + dizocilpine) was not significantly different from the unlabeled dizocilpine concentration. In this regard, final concentrations ranged between 0.1 and 4 μM and between 2 and 200 μM, for the experiments with AChRs in the desensitized (with CCh) or resting (without CCh) state, respectively. To obtain the nonspecific [³H]dizocilpine binding, a set of tubes was prepared in parallel in the presence of 200 μM proadifen (desensitized state experiments) or 500 μM dizocilpine (resting state experiments). The suspensions were equilibrated for 1 h at RT. Then, bound ([B]) dizocilpine was separated from the free ([F]) ligand by centrifugation at 18,000 rpm for 1 h. After centrifugation, 50-μl aliquots of the supernatant were removed and assayed for total radioactivity in 3 ml of Bio-Safe II. The remainder of the supernatant was aspirated, the tubes were inverted, allowed to drain for 30 min, and then wiped with cotton swabs. The pellets were resuspended in 100 μl of 10% SDS, transferred to scintillation vials with 3 ml of Bio-Safe II, and the radioactivity determined. In addition, experiments using ¹²⁵I-dizocilpine were performed basically in the same way. However, ¹²⁵I-dizocilpine was found to nonspecifically stick to Eppendorf tubes in an extent that depended on the used concentration. Thus, several experimental details were introduced to improve the accuracy of the K_d determination: a whole set of control samples without AChR membranes was used in parallel to determine the percentage of nonspecific binding, the incubation procedure was done using glass test tubes, and the centrifugation step was performed using siliconized Eppen-

dorf tubes (Fisher Scientific, Pittsburgh, PA). Finally, the radioactivity in the supernatants and in the pellets were directly determined using the gamma counter.

Binding data were fitted to the Rosenthal-Scatchard plot (Scatchard, 1949) by using the equation:

$$[B]/[F] = ([B]/K_d) + (B_{max}/K_d) \tag{3}$$

where B_{max}, the number of dizocilpine binding sites, can be estimated from the x-intersect of the plot [B]/[F] versus [B]. Thus, the number of dizocilpine binding sites per receptor is calculated considering the used concentration of AChRs (0.3 μM) and summarized in Table 1. The K_d value of dizocilpine is obtained from the negative reciprocal of the slope and summarized in Table 1.

Photoaffinity Labeling of AChR with ¹²⁵I-Dizocilpine. To photolabel the AChR with ¹²⁵I-dizocilpine in the desensitized or resting state, approximately 0.2 μM AChR native membranes was resuspended in VDB with 2.3 nM ¹²⁵I-dizocilpine. Then, the total volume was divided into different glass test tubes without or with either 0.4 mM CCh (desensitized) or 5 μM α-BTx (resting) and incubated in the dark for 1 h at RT. After reaching equilibrium, ¹²⁵I-dizocilpine was photoactivated under UV light for 7 min with a 254-nm lamp (Spectroline EN-280L; Spectronics, Westbury, NY) settled at a distance of <1 cm from the sample. The photolabeled samples were centrifuged for 1 h at 18,000 rpm. The photolabeled pellets were solubilized in Laemmli buffer and polypeptides resolved by SDS-PAGE (Laemmli, 1970). For analytical labelings, 1.0-mm-thick SDS-PAGE gels were used (1.5 mm thick for preparative labeling experiments). After electrophoresis, gels were stained with Coomassie Blue to visualize AChR subunit bands. Analytical gels were dried and exposed to X-OMAT LS sensitive films with an intensifying screen for 1 week at −80°C. The extent of photolabeling was assessed cutting out the AChR bands and determining the amount of ¹²⁵I cpm present in each band by counting in a gamma counter (10-min counting time/band). Preparative gels and analytical gels for which receptor subunits were to be subjected to proteolytic mapping were soaked in distilled water overnight, and the α1, β1, γ, and δ subunits excised from the gels. Proteolytic mapping of the sites of ¹²⁵I-dizocilpine photoincorporation within AChR subunits was performed according to the method of Cleveland et al. (1977) and as described in detail in Blanton et al. (1998). The gel suspensions were then filtered through Whatman No. 1 paper and concentrated using a Centriprep-10 (Amicon, Beverly, MA). Excess SDS was removed by acetone precipitation (~85% acetone at −20°C for 12 h).

Isolation of ¹²⁵I-Dizocilpine-Photolabeled Fragments of the AChR α1 subunit. The analytical gel containing the AChR subunits photolabeled with ¹²⁵I-dizocilpine in the absence or in the presence of CCh was soaked in water overnight. The AChR α1 subunit from each condition was excised and the gel pieces soaked in overlay buffer for 20 min (Cleveland et al., 1977). The gel pieces were then transferred to the well of a 15% acrylamide mapping gel and overlaid with 15 μl of 0.4 μg/μl *Staphylococcus aureus* V8 protease (0.6 μg). After electrophoresis, gels were stained, destained, dried, and exposed to Kodak X-OMAT LS sensitive films with an intensifying screen for 3 weeks at −80°C.

Alternatively, AChR α1 subunits photolabeled with ¹²⁵I-dizocilpine in the absence or in the presence of CCh were excised from preparative gels. For digestion with trypsin, acetone-precipitated α1 subunits were resuspended in approximately 300 μl of 0.1 M NH_4HCO_3, 0.1% (w/v) SDS, 0.5% Genapol C-100, pH 7.8. Trypsin was added at a 20% (w/w) enzyme to substrate ratio, and the digestion was allowed to proceed 4 to 5 days at RT. A small aliquot of each sample was electrophoresed on an analytical 16.5% T, 6% C Tricine SDS-PAGE gel with at least one reference lane containing prestained low molecular weight protein standards (Life Technologies, Inc., Gaithersburg, MD). The Tricine gel was stained, destained, and dried for auroradiography. The bulk of the α1 sub-

units tryptic digests were separated by reversed-phase HPLC as described in Blanton et al. (2000).

Results

Equilibrium Binding of [³H]Dizocilpine in the AChR Desensitized and Resting State. The existence of saturable binding for dizocilpine, defined as the amount of [³H]dizocilpine bound that is displaced by an excess (200 μM) of unlabeled proadifen, was demonstrated in AChR-rich membranes from *T. californica* electric organ in the presence of
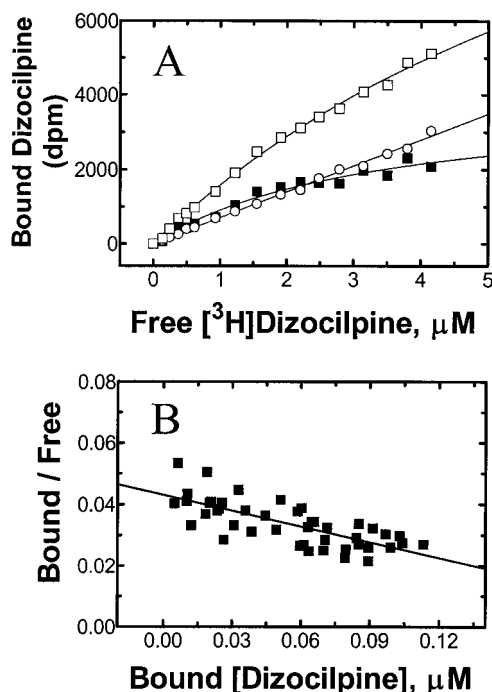
Fig. 1. [³H]Dizocilpine binding to AChR-rich membranes in the desensitized state. A, total (□), nonspecific (○), and specific (■) [³H]dizocilpine binding. AChR-rich membranes (0.3 μM) were equilibrated (1 h) with increasing concentrations of [³H]dizocilpine (0.1–4.0 μM) in the presence of CCh (1 mM). The AChR membranes were then centrifuged and the radioactivity of the pellets were measured as described under *Experimental Procedures*. The nonspecific radioactivity was determined with proadifen (200 μM). Specific or proadifen-sensitive [³H]dizocilpine binding is defined as total minus the nonspecific [³H]dizocilpine binding. B, Rosenthal-Scatchard plots for [³H]dizocilpine specific binding. The K_d values were determined from the negative reciprocal of the slope of three separate experiments according to eq. 3, and then averaged, and finally summarized in Table 1. This plot is the result of three different experiments.

TABLE 1
Dissociation constant (K_d) and stoichiometry of dizocilpine binding to AChRs in the desensitized and resting state

K_d values in the AChR-desensitized state were obtained from the negative reciprocal of the slope of Fig. 1B, according to eq. 3. The values in the resting state were estimated from a similar plot (data not shown). Number of dizocilpine binding sites per AChR in the desensitized state was obtained from the *x*-intersect of Fig. 1B, according to eq. 3, and considering the used receptor concentration (0.3 μM). The stoichiometry in the resting state was estimated from a similar plot (data not shown).

AChR State	K_d	Stoichiometry
	μM	*binding sites/AChR*
Desensitized	4.8 ± 1.0	0.72 ± 0.05
	5.4 ± 0.8[a]	
Resting	~140	3–6

[a] This value was obtained from ¹²⁵I-dizocilpine binding experiments (data not shown).

CCh. Figure 1A shows the total, nonspecific, and specific [³H]dizocilpine binding to AChR native membranes. Figure 1B shows the Rosenthal-Scatchard plot for this specific binding. These experimental results indicate the existence of one (0.72 ± 0.05 site/AChR) high-affinity (K_d = 4.8 ± 1.0 μM) dizocilpine binding site on the muscle-type AChR when the receptor is in the desensitized conformational state (Table 1). Nearly the same K_d (5.4 ± 0.8 μM) was obtained from ¹²⁵I-dizocilpine binding experiments (Table 1). Additional experiments demonstrate that dizocilpine inhibits the binding of either the high-affinity NCI [³H]TCP (Fig. 2) or [³H]dizocilpine (data not shown) to desensitized AChRs with K_i values of 7.0 ± 0.8 and 3.3 ± 0.2 μM, respectively (Table 2). These values are in agreement with our previous K_d values obtained from equilibrium binding experiments (Table 1).

In an attempt to study [³H]dizocilpine binding in the AChR resting state (without CCh), we used higher concentrations of [³H]dizocilpine and 500 μM unlabeled dizocilpine to obtain the nonspecific binding. Nevertheless, we observed a very low specific binding. Thus, the K_d values and the stoichiometry were very difficult to calculate accurately. However, we estimated that the AChR in the resting state bears between 3 and 6 low-affinity (K_d = ~140 μM) dizocilpine binding sites (Table 1).

From control experiments it was also determined that dizocilpine does not interact to the agonist binding sites (data not shown), which is in agreement with previous observations (Ramoa et al., 1990; Amador and Dani, 1991).

Dizocilpine-Induced Inhibition of NCI Binding to Their Respective High-Affinity Sites on the AChR. Previous studies show that dizocilpine increases the IC_{50} value for the high-affinity NCI [³H]histrionicotoxin (HTX) (Ramoa et al., 1990). We now demonstrate that dizocilpine effectively displaces other NCIs such as [³H]TCP (Fig. 2), quinacrine (Fig. 3A), ethidium (Fig. 4A), and CrV (Fig. 5A) from their respective high-affinity binding sites on the desensitized AChR. To compare the effect of dizocilpine on either quinacrine, ethidium, or CrV, their respective K_d values were determined in the absence and in the presence of increasing concentrations of dizocilpine. Examples of the results of a set of these titrations are shown in part A of Figs. 3–5. These figures show typical NCI titrations performed in duplicate as
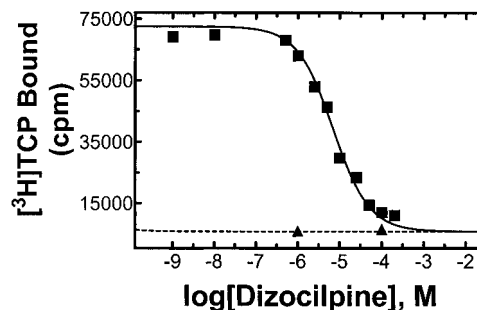
Fig. 2. Dizocilpine-induced displacement of [³H]TCP binding to desensitized AChRs. AChR-rich membranes (0.2 μM) were equilibrated (1 h) with [³H]TCP (~6 nM) and CCh (0.4 mM), in the presence of increasing concentrations of dizocilpine (0.01–200 μM). The AChR membranes were then centrifuged and the radioactivity of the pellets were measured as described under *Experimental Procedures*. The nonspecific radioactivity was determined with 200 μM proadifen (▲). The IC_{50} value was calculated by nonlinear least-squares fit with one component. The K_i value for dizocilpine was calculated using this IC_{50} value according to eq. 2 and is summarized in Table 2.
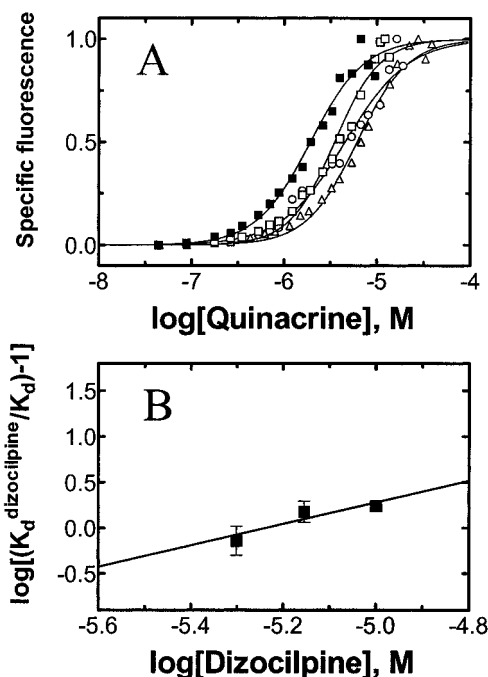
the specific (or proadifen-sensitive) fluorescence of quinacrine, ethidium, or CrV when binding to the AChR in the presence of CCh. The plots were best fit by nonlinear regression with a single component.

In the presence of dizocilpine, the apparent K_d value of quinacrine was increased to a higher extent than the apparent K_d values of ethidium and CrV. To determine the apparent K_i value of dizocilpine from the elicited displacement on either AChR-bound fluorescent NCI, Schild plots were constructed (part B of Figs. 3–5). The K_i values in the AchR-desensitized state, obtained from the antilog of the x-intercept, were found to be 5.8, 11.9, and 119 μM, for the displacement of quinacrine, CrV, or ethidium, respectively, and are summarized in Table 2. The K_i values obtained from the displacement of quinacrine or CrV from its high-affinity binding site are in good accordance with the dizocilpine K_d value obtained by equilibrium binding (Table 1), whereas the K_i value obtained from dizocilpine-induced inhibition of ethidium binding is much higher than the dizocilpine K_d. Because the slopes from the ethidium and CrV Schild plots are different from 1 (Table 2), the calculated K_i values should be considered "apparent K_i values". Instead, the calculated K_i value for quinacrine is the only one that can be considered a true K_i value because the slope from the Schild plot is near unity.

Taking advantage of the fact that CrV binds with high affinity to AChRs in the resting state (Lurtz and Pedersen, 1999), we measure the CrV K_d value by direct fluorescent titrations (Fig. 6A). In this case, the CrV K_d value in the resting state was 0.63 $\pm$ 0.28 μM ($n = 8$), a value ~6-fold higher than in the desensitized state (103 $\pm$ 26 nM; $n = 5$),. This ratio is similar (~10-fold) to that found by Lurtz and Pedersen (1999). Experiments in parallel, demonstrate that dizocilpine also displaces CrV from its binding site on the AChR in the resting state (Fig. 6A). The dizocilpine K_i value obtained from the Schild plot shown in Fig. 6B, is also summarized in Table 2. The apparent K_i value is on the same order (284 μM) as the dizocilpine K_d value calculated by equilibrium binding (Table 1).

To determine the mechanism of inhibition (steric versus allosteric) for the dizocilpine-induced displacement experiments, the slopes from the Schild plots (part B of Figs. 3–6) were calculated and summarized in Table 2. In general, values of 1 or near unity suggest a steric mode of displacement, whereas values higher or lower than 1 suggest an allosteric inhibitory mechanism. In this regard, whereas the dizocilpine-induced displacement of ethidium or CrV from its

Fig. 3. Dizocilpine-induced inhibition of quinacrine binding to its high-affinity site on the desensitized AChR. A, specific (proadifen-sensitive) fluorescence of quinacrine in the absence (■) or in the presence of 5 (□), 7 (○), or 10 μM dizocilpine (△). Quinacrine was directly titrated into AChR-containing membranes (0.3 μM) in the presence of CCh (1 mM), and in the absence (control) or in the presence of dizocilpine at ~30°C. Proadifen (200 μM) was used to determine the nonspecific fluorescence. Estimates of the apparent K_d values were made by fitting plots of the specific changes in quinacrine fluorescence versus the added ligand concentration to the equation for a sigmoid curve. These plots are the average of an experiment preformed in duplicate and are examples of at least four separate determinations. The quinacrine K_d value in control conditions (without dizocilpine) is 4.0 $\pm$ 1.8 μM ($n = 14$). B, Schild plot for the effect of dizocilpine on the apparent K_d value of quinacrine. The dizocilpine K_i value is obtained from the antilog of the x-intercept according to eq. 1 and is summarized in Table 2. The slope of this plot is also summarized in Table 2.
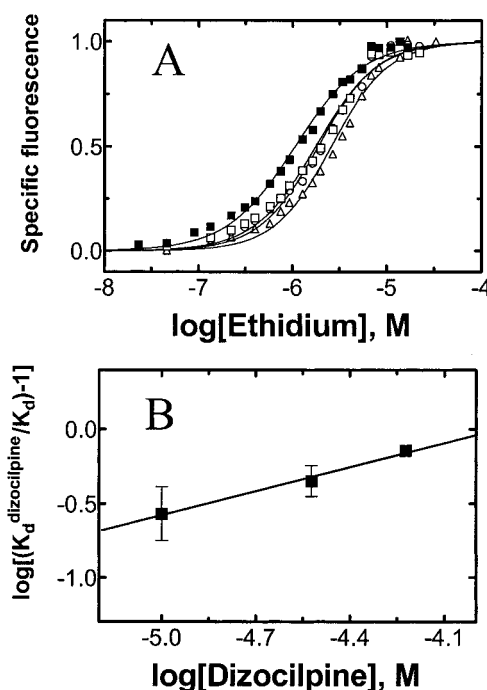
Fig. 4. Dizocilpine-induced inhibition of ethidium binding to its high-affinity site on the desensitized AChR. A, specific (proadifen-sensitive) fluorescence of ethidium in the absence (■) or in the presence of 10 (□), 30 (○), or 60 μM dizocilpine (△). Ethidium was directly titrated into AChR-containing membranes (0.3 μM) in the presence of CCh (1 mM), and in the absence (control) or in the presence of dizocilpine at ~30°C. Proadifen (200 μM) was used to determine the nonspecific fluorescence. Estimates of the apparent K_d values were made by fitting plots of the specific changes in ethidium fluorescence versus the added ligand concentration to the equation for a sigmoid curve. These plots are the average of an experiment preformed in duplicate and are examples of at least three separate determinations. The ethidium K_d value in control conditions (without dizocilpine) is 1.6 $\pm$ 0.2 μM ($n = 5$). B, Schild plot for the effect of dizocilpine on the apparent K_d value of ethidium. The dizocilpine K_i value is obtained from the antilog of the x-intercept according to eq. 1 and is summarized in Table 2. The slope of this plot is also summarized in Table 2.
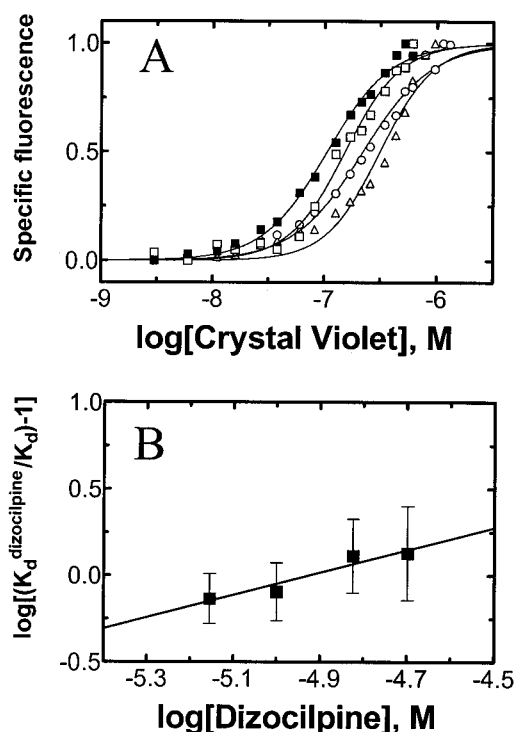
high-affinity binding site on the desensitized AChR seems to be mediated by an allosteric mechanism (slopes of 0.54 ± 0.20 and 0.65 ± 0.50, respectively), the displacement of quinacrine is mediated by a steric mechanism (slope = 1.18 ± 0.51). In addition, the slope (2.93 ± 1.20) from Fig. 6B, which is also summarized in Table 2, indicates that dizocilpine inhibits CrV binding to AChRs in the resting state by an allosteric mode of action.

The K_i value obtained from the inhibition of ^{125}I-dizocilpine binding (18.4 ± 1.5 μM; Table 2) by the intracellular calcium antagonist TMB-8 (Fig. 7A) is higher than that obtained from the inhibition of [3H]dizocilpine (8.7 ± 1.2 μM; Table 2). This might be due to the observed nonspecific binding of ^{125}I-dizocilpine to plastic tubes. The TMB-8-induced inhibition of [3H]TCP binding gave practically the same result (3.1 ± 0.2 μM; Table 2) as previous experiments performed in our laboratory using [3H]PCP (2.4 ± 0.1 μM; Sun et al., 1999).

Characterization of [125I]Dizocilpine Photoincorporation into AChR. Initial photolabeling experiments with ^{125}I-dizocilpine were designed to characterize the extent of photoincoproration into AChR subunits, as well as to assess the extent to which the addition of cholinergic ligands (CCh

or α-BTx) affect the extent of ^{125}I-dizocilpine photoincorporation into AChR subunits. The extent of photoincorporation into the AChR was monitored by autoradiography after SDS-PAGE of the solubilized membrane pellets. As is evident in the autoradiographs shown in Fig. 8A, there is significant photoincorporation of ^{125}I-dizocilpine into the α1 subunit. Minor photoincorporation into the AChR β1, γ, and δ subunits is evident in autoradiographs of greater length of exposure (4 weeks), along with increased background exposure (data not shown). To quantify the extent of photoincorporation into each AChR subunit, the gel bands were excised and ^{125}I cpm determined by gamma-counting. From these experiments the extent of photoincorporation into the α1, β1, γ, and δ subunits was 77 ± 5, 21 ± 1, 28 ± 2, and 24 ± 2 cpm/μg, respectively, which results in a stoichiometry of 2(α1):0.55(β1):0.73(γ):0.63(δ) and a molar labeling efficiency into α1 of approximately 0.01%. This is in reasonably good agreement with the stoichiometry of the *T. californica* AChR [2(α1):1(β1):1(γ):1(δ)].

There is also considerable photoincorporation into the α subunit (α_{NK}) of the Na$^+$,K$^+$-ATPase (Fig. 8A). The fact that dizocilpine interacts with a lipid membrane-embedded protein is in agreement with the lipophilic nature of the dizo-


Fig. 5. Dizocilpine-induced inhibition of crystal violet binding to its high-affinity site on the desensitized AChR. A, specific (proadifen-sensitive) fluorescence of CrV in the absence (■) or in the presence of 7 (□), 15 (○), or 20 μM dizocilpine (△). Crystal violet was directly titrated into AChR-containing membranes (0.3 μM) in the presence of CCh (1 mM), and in the absence (control) or in the presence of dizocilpine at ~30°C. Proadifen (200 μM) was used to determine the nonspecific fluorescence. Estimates of the apparent K_d values were made by fitting plots of the specific changes in CrV fluorescence versus the added ligand concentration to the equation for a sigmoid curve. These plots are the average of an experiment preformed in duplicate and are examples of at least four separate determinations. The CrV K_d value in control conditions (without dizocilpine) is 103 ± 26 nM (n = 5). B, Schild plot for the effect of dizocilpine on the apparent K_d value of CrV. The dizocilpine K_i value is obtained from the antilog of the x-intercept according to eq. 1 and is summarized in Table 2. The slope of this plot is also summarized in Table 2.
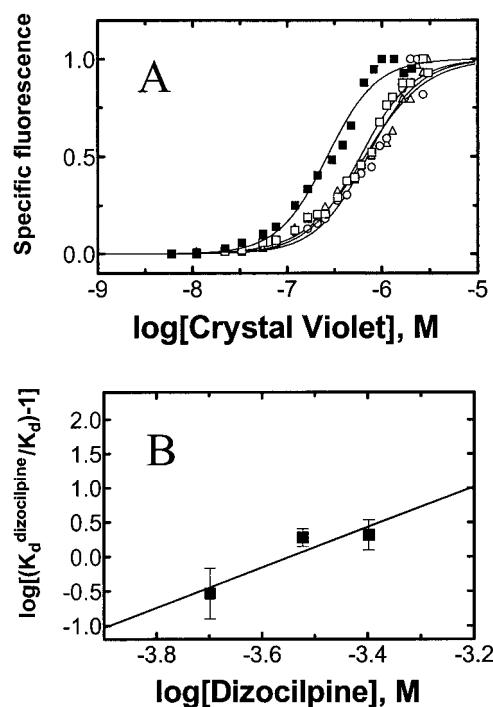
Fig. 6. Dizocilpine-induced inhibition of crystal violet binding to its high-affinity site on the AChR in the resting state. A, specific (PCP-sensitive) fluorescence of CrV in the absence (■) or in the presence of 200 (■), 300 (○), or 400 μM dizocilpine (△). Crystal violet was directly titrated into AChR-containing membranes (0.3 μM) in the absence of CCh, and in the absence (control) or in the presence of dizocilpine at ~30°C. Phencyclidine (100 μM) was used to determine the nonspecific fluorescence. Estimates of the apparent K_d values were made by fitting plots of the specific changes in CrV fluorescence versus the added ligand concentration to the equation for a sigmoid curve. These plots are the average of an experiment preformed in duplicate and are examples of at least three separate determinations. The CrV K_d value in control conditions (without dizocilpine) is 0.63 ± 0.28 μM (n = 8). B, Schild plot for the effect of dizocilpine on the apparent K_d value of CrV. The dizocilpine K_i value is obtained from the antilog of the x-intercept according to eq. 1 and is summarized in Table 2. The slope of this plot is also summarized in Table 2.
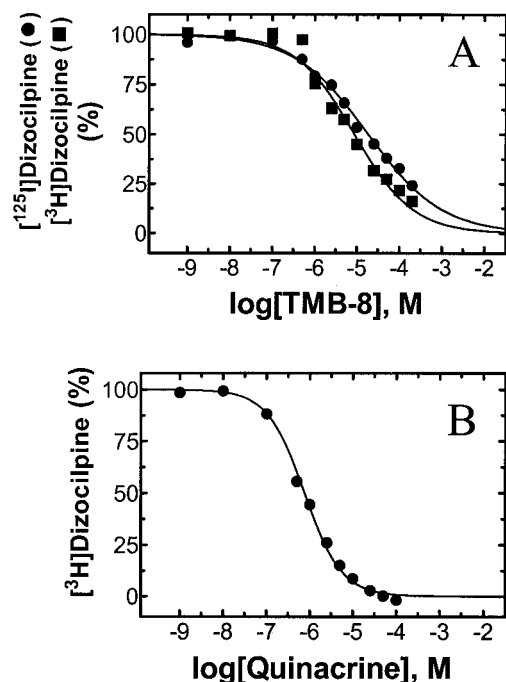
Fig. 7. TMB-8- and quinacrine-induced displacement of [³H]dizocilpine binding to desensitized AChRs. A, TMB-8-induced displacement of [³H] or ¹²⁵I-dizocilpine binding to desensitized AChRs. AChR-rich membranes (0.2 μM) were equilibrated (2.5 h) with [³H]dizocilpine (~36 nM) or ¹²⁵I-dizocilpine (~0.7 nM) and CCh (0.4 mM), in the presence of increasing concentrations of TMB-8 (0.001–200 μM). Because these plots did not fit by nonlinear least-squares and Hill coefficients of 1, the IC₅₀ values were calculated by fitting these plots with fixed Hill coefficients of less than unity (Table 2). The K_i value for TMB-8 was calculated using this IC₅₀ value according to eq. 2 and summarized in Table 2. B, quinacrine-induced displacement of [³H]dizocilpine binding to desensitized AChRs. AChR-rich membranes (0.2 μM) were equilibrated (2.5 h) with [³H]dizocilpine (15 nM) and CCh (0.4 mM), in the presence of increasing concentrations of quinacrine (0.001–200 μM). In both cases, the AChR membranes were then centrifuged and the radioactivity of the pellets were measured as described under *Experimental Procedures*. The nonspecific radioactivity was determined with proadifen (200 μM).

TABLE 2

Inhibition constant (K_i) for dizocilpine and TMB-8 determined by the inhibition of either binding or photolabeling of NCIs to their respective sites on AChRs in the desensitized or resting conformational state

K_i values for dizocilpine using quinacrine, ethidium, and CrV displacement binding were obtained from the Schild plots shown in part B of Figs. 3–6, according to eq. 1. The other K_i values for dizocilpine were calculated using the Cheng-Prusoff relationship (eq. 2) and the IC₅₀ values obtained from Fig. 2 ([³H]TCP) and from data not shown for [¹²⁵I]TID and [³H]dizocilpine. K_i values for TMB-8 were also calculated using the Cheng-Prusoff relationship (eq. 2) and the IC₅₀ values obtained from Fig. 7A ([³H] and ¹²⁵I-dizocilpine) and from data not shown for [³H]TCP. The slope values for quinacrine, ethidium, and crystal violet are from the Schild plots shown in part B of Figs. 3–6, respectively. The remaining slope values, obtained from the slopes of the competition experiments shown in Fig. 2 ([³H]TCP), Fig. 7A (TMB-8), and for data not shown, are the Hill coefficients (n_H).

NCI	K_i		Slope
	Desensitized	Resting	
	μM		
Quinacrine	5.8		1.18 ± 0.51
Ethidium	119		0.54 ± 0.20
Crystal violet	11.9		0.56 ± 0.50
		284	2.93 ± 1.20
[¹²⁵I]TID		197 ± 25	1.19 ± 0.14
[³H]TCP	7.0 ± 0.8		0.93 ± 0.08
[³H]Dizocilpine	3.3 ± 0.2		0.93 ± 0.04
¹²⁵I-Dizocilpine	18.4 ± 1.5		0.50 ± 0.02
[³H]Dizocilpine	8.7 ± 1.2		0.62 ± 0.05
[³H]TCP	3.1 ± 0.2		0.88 ± 0.05

cilpine molecule. The α subunit of the Na⁺,K⁺-ATPase has also been photolabeled with other hydrophobic probes such as [¹²⁵I]TID and its derivatives (Blanton et al., 2000), [³H]tetracaine (Middleton et al., 1999), and [³H]ethidium diazide (Pratt et al., 2000).

Addition of agonist leads to a slight reduction in the extent of ¹²⁵I-dizocilpine photoincorporation into each subunit, with the greatest reduction observed in the α1-(~10%) and γ subunit (~14%). On the contrary, addition of the competitive antagonist α-BTx (5 μM) or the potent local anesthetic and NCI proadifen (0.1–200 μM concentration range, with or without CCh) has no effect on the extent of photoincorporation into any subunit (data not shown). For instance, one experiment showed an extent of incorporation into the α1 subunit of 85 ± 12 and 85 ± 5 cpm/μg, in the absence or in the presence of α-BTx, respectively.

¹²⁵I-Dizocilpine photoincorporation into the AChR α1 subunit labeled in the absence or in the presence of agonist was further characterized by proteolytic mapping. The α1 subunit (with or without CCh) was partially digested using *S. aureus* V8 protease under Cleveland gel conditions (Cleveland et al., 1977; Blanton et al., 2000). Cleveland gel analysis of the α1 subunit generates four large, nonoverlapping fragments of the α1 subunit allowing the distribution of the ¹²⁵I cpm within the subunit to be determined (Blanton et al., 1998). Photoincorporation into the α1 subunit is restricted to two V8 protease fragments, α1V8-20 (Ser¹⁷³-Glu³³⁸) and α1V8-10 (Asn³³⁹-Gly⁴³⁷) (Fig. 8B). The stretch of the primary sequence of the α1 subunit contained within V8 protease segment V8-20 includes the transmembrane fragments M1, M2, and M3; the fragment V8-10 contains the transmembrane segment M4. The percentage of the total ¹²⁵I-dizocilpine photoincorporation into the α1 subunit found in V8-20 and V8-10 was 29 ± 7 and 71 ± 7%, respectively. The extent of ¹²⁵I-
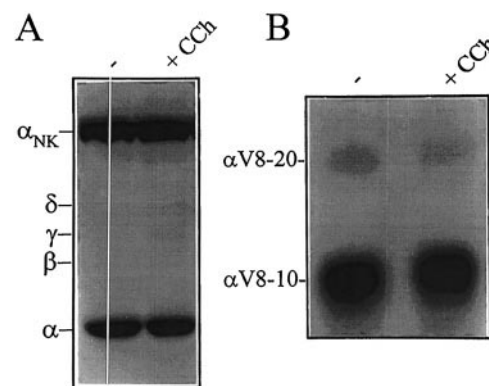
Fig. 8. Photoincorporation of ¹²⁵I-dizocilpine into AChR-rich membranes in the resting and desensitized state of the AChR. AChR-rich membranes (0.2 μM) were equilibrated (1 h) with ¹²⁵I-dizocilpine (~2.3 nM) in the absence (− lane) or in the presence of 0.4 mM CCh (+ lane) and then irradiated at 254 nm for 7 min (at a distance of <1 cm). A, photolabeled AChR subunits were resolved by SDS-PAGE, visualized by Coomassie Blue staining, and subjected to autoradiography (1-week exposure with intensifying screen). Labeled lipids and free photolysis products were electrophoresed from the gel with the tracking dye. The migration of individual AChR subunits is indicated on the left. The α subunit of the Na⁺, K⁺-ATPase (α_NK) is also indicated. B, mapping the sites of ¹²⁵I-dizocilpine into the AChR α1 subunit. The ¹²⁵I-dizocilpine-labeled α1 subunit isolated from AChRs labeled in the resting (− lane) and desensitized state (+ lane) were partially digested with V8 *S. aureus* protease as described under *Experimental Procedures*. The labeled fragments (V8-10 and V8-20) were resolved by SDS-PAGE (15% polyacrylamide gel) and subjected to autoradiography.

dizocilpine photoincorporation into the protease fragment α1V8-10 was only slightly altered when the labeling was conducted in the presence and absence of agonist (168 ± 11 and 192 ± 12 cpm, respectively). No significant difference (>10%) in the extent of ^{125}I-dizocilpine photoincorporation into α1V8-20 was observed. The results indicate that the extent of ^{125}I-dizocilpine photoincorporation into the α1 subunit is insensitive to the conformational changes elicited by the presence of agonists (i.e., resting to desensitized state).

To further localize the site of ^{125}I-dizocilpine labeling within the fragments α1V8-20 and α1V8-10, each fragment was ezymatically digested with trypsin. When an aliquot of each digest was resolved by Tricine SDS-PAGE, for α1V8-20 a single labeled fragment was visualized by autoradiography migrating with an apparent molecular mass of 4 kDa and for α1V8-10 there were two labeled bands of ~4 and 5 kDa. The bulk of the tryptic digests were separated by reversed-phase HPLC (Fig. 9). For each digest a single cpm peak of ^{125}I and corresponding peak of absorbance were evident. HPLC fractions 37 to 39 and 40 to 42 were pooled for the digest of α1V8-20 (Fig. 9A) and α1V8-10 (Fig. 9B), respectively, and subjected to amino-terminal amino acid sequence analysis. For α1V8-10 (HPLC fractions 40–42) sequence analysis revealed the presence of two peptides one beginning at Ser[388] and the other at Tyr[401]. Based on apparent molecular masses of 4 and 5 kDa, that were estimated from an analytical Tricine gel, each peptide would extend through the transmembrane segment M4 (Asp[407]–Arg[429]) and terminate at the carboxyl terminus of the α- subunit (Gly[437]). For α1V8-20

(HPLC fractions 37–39) sequence analysis revealed the presence of a single peptide beginning at Ile[210]. A 4-kDa peptide starting at Ile[210] would extend through the transmembrane segment M1 (Arg[209]–Tyr[234]) and terminate at the beginning of the M2 segment (Lys[242]).

Discussion

We used three different experimental strategies to localize the binding site(s) for the dissociative anesthetic dizocilpine on the muscle-type AChR. First, we determined the K_d value and the number of binding sites of [3H]dizocilpine when the receptor is in the desensitized or in the resting state, respectively. Second, we calculated the apparent K_i value of dizocilpine from binding displacement experiments using NCIs that bind to different high-affinity sites on the AChR when it is in the desensitized or resting conformational state, respectively. Third, we partially resolved the structural components for dizocilpine action on the AChR by photoaffinity labeling and subsequent protease degradation and amino-terminal sequence analysis.

From the first set of experiments, we found that the dizocilpine K_d values are in the same concentration range as that found for dizocilpine-induced inhibition of either agonist-induced ion channel opening (IC$_{50}$ = ~7 μM at 0 mV; Amador and Dani, 1991) or [3H]HTX binding in the desensitized state (IC$_{50}$ = 13 ± 2 μM; Ramoa et al., 1990). In addition, various neuronal-type AChRs are reported to be inhibited by dizocilpine at concentrations that depend on the receptor type ranging from 1 to 36 μM (Briggs and McKenna, 1996; Buisson and Bertrand, 1998; Halliwell et al., 1989; Ramoa et al., 1990; Yamakura et al., 2000). Specifically, receptors containing β4 subunits (IC$_{50}$ = 2.7–8.5 μM) were more sensitive to dizocilpine than those containing β2 subunits (IC$_{50}$ = 20–36 μM), and α3-composed receptors were more sensitive than those containing the α2, α4, or α7 (IC$_{50}$ = 15 ± 3 μM) subunit (Briggs and McKenna, 1996; Yamakura et al., 2000). In this regard, our K_d values are similar to those obtained for the α4β4 neuronal-type AChRs (IC$_{50}$ = 4.5 μM; Yamakura et al., 2000).

The observed stoichiometry for dizocilpine binding in the desensitized state is in accord with previous data for other NCIs indicating one high-affinity binding site per AChR (for review, see Arias, 1998, 1999b). Hill coefficients (n_H) of 0.93 ± 0.08 and 0.93 ± 0.04 (Table 2), obtained from dizocilpine-induced inhibition of [3H]TCP (Fig. 2) or [3H]dizocilpine (data not shown) binding experiments, respectively, support the existence of one high-affinity noncooperative binding site in the desensitized AChR. The dose-inhibition relations for dizocilpine on several neuronal-type AChRs gave n_H values of 0.9 to 1.1 (Yamakura et al., 2000), which also suggests one binding site per AChR.

We also estimated that dizociline binds with low affinity (K_d = ~140 μM) to three to six binding sites on the AChR in the resting state. The fact that dizocilpine inhibits [^{125}I]TID photolabeling (data not shown) and CrV binding (Fig. 6) to AChRs in the resting state with K_i values of 197 and 284 μM (Table 2) supports our binding results. In addition, the observed values are in agreement with the IC$_{50}$ obtained from dizocilpine-induced inhibition of [3H]HTX binding in the resting state (102 ± 12 μM; Ramoa et al., 1990). Although there is no previous evidence for the stoichiometry of the
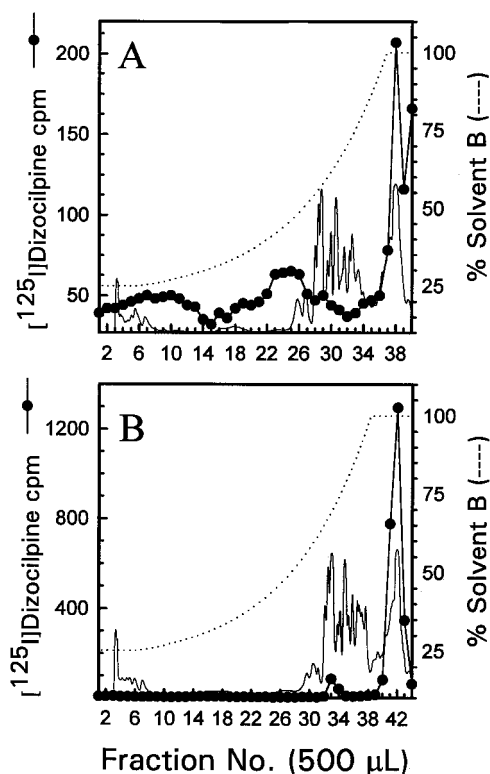
Fig. 9. Reverse phase HPLC separation of tryptic digests of ^{125}I-dizocilpine-labeled α1V8-20 and α1V8-10. Tryptic digests of ^{125}I-dizocilpine-labeled α1V8-20 (A) and α1V8-10 (B) separated by reverse phase HPLC as described under *Experimental Procedures*. The elution of peptides was monitored by absorbance at 210 nm (solid line) and elution of ^{125}I by gamma-counting of each 500-μl fraction (●).

low-affinity dizocilpine binding sites on the AChR in the resting state, a similar number (3.7 ± 1.5) of low-affinity binding sites for PCP, another dissociative anesthetic, was found in the same AChR type (Arias, 1999a). The low-affinity PCP binding sites have been suggested to be located at the nonannular lipid domain of the desensitized AChR.

Taking into account the observed K_i values for dizocilpine obtained from displacement of AChR-bound quinacrine, ethidium, or CrV from its respective high-affinity binding site on the AChR, we can affirm that dizocilpine specifically inhibits the binding of quinacrine or CrV to desensitized AChRs or the binding of CrV to AChRs in the resting state. Instead, ethidium binding is inhibited by dizocilpine at very high concentrations. Considering that the ethidium binding site is located in the ion channel (Herz et al., 1989) and that ethidium diazide photolabeled both M1 and M2 (e.g., α1Leu[251] and α1Ser[252]) segments (Pratt et al., 2000), we may conclude that the dizocilpine binding site is not located in the ion channel lumen. On the other hand, Schild-type analyses indicate that dizocilpine inhibition of CrV binding when the AChR is in the desensitized or resting conformational state is mediated by an allosteric mechanism. Although there is not direct evidence for the localization of the CrV binding site, indirect evidence (i.e., CrV specifically displaced the high-affinity NCI PCP) supports a luminal ion channel localization (Lurtz and Pedersen, 1999). Again, the experimental evidence suggests that the dizocilpine binding site is not located in the ion channel when the AChR is in the desensitized or in the resting conformational state. Interestingly, Schild-type analyses also indicate that the inhibition of quinacrine binding is probably mediated by a steric mechanism. Considering that the high-affinity binding site for quinacrine (for review, see Arias, 1998) is located apart from the ion channel (Valenzuela et al., 1992; Arias et al., 1993b), probably in a nonannular lipid domain of the desensitized AChR (Arias, 1997) ~12 Å from the lipid-water interface (Arias et al., 1993a), we may conclude that the high-affinity dizocilpine binding site is located in a nonannular lipid domain near the quinacrine locus. The exact location for the nonannular lipid domain on the AChR is unkown. However, indirect determinations have suggested that this domain may be located between the five subunits (two α1, one β1, one γ, and one δ) of the AChR and/or between the crevices formed by the interaction of the four transmembrane domains (M1–M4) from each subunit (Jones and McNamee, 1988; for review, see Arias, 1998, 1999b).

In general, the results from TMB-8-induced inhibition of [³H] or ¹²⁵I-dizocilpine and [³H]TCP binding experiments (Fig. 7; Table 2) are in good agreement with the IC_{50} value for TMB-8 obtained in α4β2 at −100 mV (17.2 ± 2.9 μM; Buisson and Bertrand, 1998). Although TMB-8-induced inhibition of [³H]dizocilpine binding was similar to [³H]PCP inhibition, the n_H values obtained from the [³H] or ¹²⁵I-dizocilpine inhibition experiments were less than 1 (0.62 ± 0.05 and 0.50 ± 0.05, respectively; Table 2), which contrasts with [³H]TCP binding inhibition experiments (data not shown) where the observed n_H value is near unity (0.88 ± 0.05; Table 2). These results suggest that TMB-8 inhibits [³H]TCP binding by a noncooperative mechanism, whereas it inhibits [³H]dizocilpine binding in a negative cooperative manner. In turn, this latter evidence suggests that TMB-8 inhibits the binding of dizocilpine by an allosteric mechanism. The pharmacolog-

ical action of TMB-8 on muscle- and neuronal-type AChRs is believed to be mediated by ion flux inhibition upon binding to the ion channel (Bencherif et al., 1995; Buisson and Bertrand, 1998; Sun et al., 1999). In this regard, the dizocilpine binding site is unlikely to be located in the ion channel. The fact that dizocilpine inhibits human α4β2 ion channels with n_H values less than 1 (0.70 ± 0.05; Buisson and Bertrand, 1998) supports a negative cooperative mode of action, probably by an allosteric mechanism, which indirectly suggests a nonluminal ion channel localization. On the other hand, either dizocilpine- or quinacrine-induced inhibition of [³H]dizocilpine binding shows an n_H value near 1 suggesting a steric mode of inhibition. This is in agreement with the possibility that the dizocilpine binding site overlaps, at least partially, the quinacrine locus.

From the third set of experiments we state that ¹²⁵I-dizocilpine photoincorporates into each AChR subunit, although principally into the α1 subunit. Within the α1 subunit the majority of ¹²⁵I-dizocilpine labeling maps to the transmembrane segment M1 and M4, demonstrating that dizocilpine binds at the lipid-protein interface of the receptor (Blanton et al., 1998), a result consistent with the lipophilic nature of the dizocilpine molecule. However, several factors indicate that some or all of the ¹²⁵I-dizocilpine labeling in the transmembrane segments M1 and M4 may not result from interaction with the high-affinity binding site on the receptor as determined by radioligand binding experiments. First, the fact that the extent of ¹²⁵I-dizocilpine incorporation into the AChR is the same in the resting and desensitized conformation is surprising given an approximately 30-fold difference in the relative dizocilpine binding affinities for each receptor conformation. Second, addition of increasing concentrations of the NCI proadifen had no effect on the extent of ¹²⁵I-dizocilpine incorporation into AChR subunits while reducing [³H]dizocilpine binding to the desensitized receptor by greater than 70%. These results suggests that the observed photolabeling of ¹²⁵I-dizocilpine is predominantly nonspecific arising from dizocilpine interaction with the AChR lipid-protein interface. Dizocilpine binding to its high-affinity site on the desensitized state may result in only a very small component of specific photoincorporation that is masked by a much larger component of nonspecific labeling at the receptor lipid-protein interface.

On the other hand, we demonstrate that there is no radioactivity associated with a fragment containing the M2 transmembrane domain of the α1 subunit, a result that is consistent with data presented in this article and elsewhere that argue against a luminal binding site for dizocilpine. However, our pharmacological experiments demonstrate that dizocilpine sterically competes for the quinacrine binding site when the AChR is in the desensitized state. In this regard, previous photolabeling experiments using quinacrine azide demonstrated that the quinacrine binding site is located in the M1 transmembrane domain of the α1 subunit at residues Arg[209] and Pro[211] (DiPaola et al., 1990). In addition to these amino acids, site-directed mutagenesis experiments included the residue α1Tyr[213] as another component of the quinacrine binding site (Tamamizu et al., 1995). In contrast, hydrophobic photolabeling studies implicate residues in α1 M1 that are located C-terminal to Pro[211] as being situated at the lipid-protein interface (Blanton et al., 1998). Our results establish ¹²⁵I-dizocilpine photoincorporation into the α1 M1

domain and therefore one possibility is that residues within M1 contribute to both the lipid-protein interface of the AChR as well as to the high-affinity dizocilpine binding site. Unfortunately, because of the low level of radioactivity associated with ^{125}I-dizocilpine photoincorporation into the $\alpha 1$ M1 domain, we were unable to determine which amino acids reacted with ^{125}I-dizocilpine using amino acid sequence analysis. We are currently exploring an alternative strategy for examining the contribution of $\alpha 1$ M1 amino acids to dizocilpine binding and action, specifically site-directed mutagenic amino acid substitutions and electrophysiological recordings to asses the effect of dizocilpine on receptor function.

Finally, the fact that dizocilpine binds the AChR closed channel with 5.3-fold higher affinity than the open channel form is inconsistent with an open-channel-blocking mechanism (Grewer and Hess, 1999; Hess et al., 2000), but supports our conclusion that the high-affinity dizocilpine binding site is located at a nonluminal site in the desensitized AChR. In this regard, our results are in agreement with an allosteric mode of inhibition for dizocilpine on the muscle-type AChR.

Considering several parameters for dizocilpine-inducing anesthesia such as administration dose, brain/plasma ratio, brain concentration in rats, and the percentage of dizocilpine molecules bound to plasma proteins, a free plasma concentration of ~ 2 μM dizocilpine during anesthesia was calculated (Yamakura et al., 2000). This concentration is slightly beyond the lowest limit of our K_d values. Thus, the characterized high-affinity dizocilpine binding site is probably not of sufficient affinity to account for any of the in vivo effects of dizocilpine.

As was outlined above, both nicotinic and NMDA receptors are structurally different. Nevertheless, the evidence depicted in this article may help to further determine the primary structural components of the dizocilpine binding site on the NMDA receptor as well as on other neuronal-type AChRs.

Acknowledgments

References

Amador M and Dani JA (1991) MK-801 inhibition of nicotinic acetylcholine receptor channels. *Synapse* **7:**207–215.

Arias HR (1997) The high-affinity quinacrine binding site is located at a non-annular lipid domain of the nicotinic acetylcholine receptor. *Biochim Biophys Acta* **1347:**9–22.

Arias HR (1998) Binding sites for exogenous and endogenous non-competitive inhibitors of the nicotinic acetylcholine receptor. *Biochim Biophys Acta* **1376:**173–220.

Arias HR (1999a) 5-Doxylstearate-induced displacement of phencyclidine from its low-affinity binding sites on the nicotinic acetylcholine receptor. *Arch Biochem Biophys* **371:**89–97.

Arias HR (1999b) Role of local anesthetics on both cholinergic and serotonergic ionotropic receptors. *Neurosci Biobehav Rev* **23:**817–843.

Arias HR (2000) Localization of agonist and competitive antagonist binding sites on nicotinic acetylcholine receptors. *Neurochem Int* **36:**595–645.

Arias HR, Valenzuela CF and Johnson DA (1993a) Transverse localization of the quinacrine binding site on the *Torpedo* acetylcholine receptor. *J Biol Chem* **268:**6348–6355.

Arias HR, Valenzuela CF and Johnson DA (1993b) Quinacrine and ethidium bind to different loci on the *Torpedo* acetylcholine receptor. *Biochemistry* **32:**6237–6242.

Bencherif M, Eisenhour CM, Prince RJ, Lippiello PM and Lukas RJ (1995) The 'calcium antagonist' TMB-8 [3,4,5-trimethoxybenzoic acid 8-(diethylamino)octyl ester] is a potent, noncompetitive, functional antagonist at diverse nicotinic acetylcholine receptor subtypes. *J Pharmacol Exp Ther* **275:**1418–1426.

Blanton MP, McCardy EA and Gallagher MJ (2000) Examining the noncompetitive antagonist-binding site in the ion channel of the nicotinic acetylcholine receptor in the resting state. *J Biol Chem* **275:**3469–3478.

Blanton MP, McCardy EA, Huggins A and Parikh D (1998) Probing the structure of the nicotinic acetylcholine receptor with the hydrophobic photoreactive probes [^{125}I]TID-BE and [^{125}I]TIDPC/16. *Biochemistry* **37:**14545–14555.

Briggs CA and McKenna DG (1996) Effect of MK-801 at the human $\alpha 7$ nicotinic acetylcholine receptor. *Neuropharmacology* **35:**407–414.

Buisson B and Bertrand D (1998) Open-channel blockers at the human $\alpha 4\beta 2$ neuronal nicotinic acetylcholine receptor. *Mol Pharmacol* **53:**555–563.

Changeux JP and Edelstein SJ (1998) Allosteric receptors after 30 years. *Neuron* **21:**959–980.

Cheng YC and Prusoff WH (1973) Relationships between the inhibition constant (K_i) and the concentration of inhibitor which causes 50 per cent inhibition (IC_{50}) of an enzymatic reaction. *Biochem Pharmacol* **22:**3099–3108.

Cleveland DW, Fischer SG, Kirschner MW and Laemmli UK (1977) Peptide mapping by limited proteolysis in sodium dodecyl sulfate and analysis by gel electrophoresis. *J Biol Chem* **252:**1102–1106.

DiPaola M, Kao PN and Karlin A (1990) Mapping the α-subunit site photolabeled by the noncompetitive inhibitor [^{3}H]quinacrine azide in the active state of the nicotinic acetylcholine receptor. *J Biol Chem* **265:**11017–11029.

Grewer C and Hess GP (1999) On the mechanism of inhibition of the nicotinic acetylcholine receptor by the anticonvulsant MK-801 investigated by laser-pulse photolysis in the microsecond-to-millisecond time region. *Biochemistry* **38:**7837–7846.

Halliwell RF, Peters JA and Lambert JJ (1989) The mechanism of action and pharmacological specificity of the anticonvulsant NMDA antagonist MK-801: a voltage clamp study on neuronal cells in culture. *Br J Pharmacol* **96:**480–494.

Herz JM, Johnson DA and Taylor P (1989) Distance between the agonist and noncompetitive inhibitor sites on the nicotinic acetylcholine receptor. *J Biol Chem* **262:**12439–12448.

Hess GP, Ulrich H, Breitinger HG, Niu L, Gameiro AM, Grewer C, Srivastava S, Ippolito JE, Lee SM, Jayaraman V, et al. (2000) Mechanism-based discovery of ligands that counteract inhibition of the nicotinic acetylcholine receptor by cocaine and MK-801. *Proc Natl Acad Sci USA* **97:**13895–13900.

Jones OT and McNamee MG (1988) Annular and nonannular binding sites for cholesterol associated with the nicotinic acetylcholine receptor. *Biochemistry* **27:**2364–2374.

Katz EJ, Cortes VI, Eldefrawi ME and Eldefrawi AT (1997) Chlorpyrifos, parathion, and their oxons bind to and desensitize a nicotinic acetylcholine receptor: relevance to their toxicities. *Toxicol Appl Pharmacol* **146:**227–236.

Krasowski MD and Harrison NL (1999) General anesthetic actions on ligand-gated ion channels. *Cell Mol Life Sci* **55:**1278–1303.

Laemmli UK (1970) Cleavage of structural proteins during the assembly of the head of bacteriophage T4. *Nature (Lond)* **227:**680–685.

Lurtz MM and Pedersen SE (1999) Aminotriarylmethane dyes are high-affinity noncompetitive antagonists of the nicotinic acetylcholine receptor. *Mol Pharmacol* **55:**159–167.

Middleton RE, Strnad NP and Cohen JB (1999) Photoaffinity labeling the *Torpedo* nicotinic acetylcholine receptor with [^{3}H]tetracaine, a nondesensitizing noncompetitive antagonist. *Mol Pharmacol* **56:**290–299.

Ortells MO and Lunt GG (1995) Evolutionary history of the ligand-gated ion-channel superfamily of receptors. *Trends Neurosci* **18:**121–127.

Pedersen SE, Dreyer EB and Cohen JB (1986) Location of ligand binding sites on the nicotinic acetylcholine receptor α subunit. *J Biol Chem* **261:**13735–13743.

Pratt MB, Pedersen SE and Cohen JB (2000) Identification of the sites of incorporation of [^{3}H]ethidium diazide within the *Torpedo* nicotinic acetylcholine receptor ion channel. *Biochemistry* **39:**11452–11462.

Ramoa AS, Alkondon M, Aracava Y, Irons J, Lunt GG, Deshpande SS, Wonnacott S, Aronstam RS and Alburquerque EX (1990) The anticonvulsant MK-801 interacts with peripheral and central nicotinic acetylcholine receptor ion channels. *J Pharmacol Exp Ther* **254:**71–82.

Scatchard G (1949) The attractions of proteins for small molecules and ions. *Ann NY Acad Sci* **51:**660–672.

Schild HO (1949) pAx and competitive drug antagonism. *Br J Pharmacol* **4:**277–280.

Sun H, McCardy EA, Machu TK and Blanton MP (1999) Characterization of interaction of 3,4,5-trimethoxybenzoic acid 8-(diethylamino)octyl ester with *Torpedo californica* nicotinic acetylcholine receptor and 5-hydroxytryptamine$_3$ receptor. *J Pharmacol Exp Ther* **290:**129–135.

Tamamizu S, Todd AP and McNamee MG (1995) Mutations in the M1 region of the nicotinic acetylcholine receptor alter the sensitivity to inhibition by quinacrine. *Cell Mol Neurobiol* **15:**427–438.

Valenzuela CF, Kerr JA and Johnson DA (1992) Quinacrine binds to the lipid-protein interface of the *Torpedo* acetylcholine receptor: a fluorescence study. *J Biol Chem* **267:**8238–8244.

Yamakura T, Chavez-Noriega LE and Harris RA (2000) Subunit-dependent inhibition of human neuronal nicotinic acetylcholine receptors and other ligand-gated ion channels by dissociative anesthetics and dizocilpine. *Anesthesiology* **92:**1144–1153.

Send reprint requests to: Hugo R. Arias, Department of Pharmacology, School of Medicine, Texas Tech University Health Sciences Center. 3601 4th St., Lubbock, TX 79430. E-mail: phrhra@ttuhsc.edu